



Review Paper

A Review of Electrospun Nanofiber Membranes

Shahram Tabe^{1,2,*}¹ Ministry of the Environment and Climate Change, 40 St. Clair Ave. West, Toronto, ON M4V 1M2, Canada² Department of Chemical Engineering and Applied Chemistry, University of Toronto, 200 College St., Toronto, ON, M5S 3E5, Canada

Article info

Received 2017-01-12
 Revised 2017-03-11
 Accepted 2017-03-13
 Available online 2017-03-13

Keywords

Electrospun nanofiber membranes
 Water treatment
 Adsorptive membranes
 Membrane distillation
 Desalination

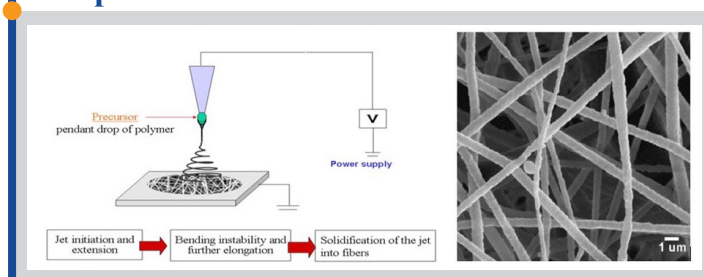
Highlights

- A new generation of membranes offering higher flux at lower applied pressure
- Highly porous with interconnected pores
- High specific surface area, suitable for adsorption applications
- Have found applications in water treatment, air cleaning, membrane distillation, among many other uses

Abstract

Electrospun nanofiber membranes (ENMs) are new generation of membranes with many favorable properties such as high flux and low pressure drop. Although electrospinning has been known for more than a century, its applications in filtration and separation processes are relatively new. Electrospinning has provided the means to produce ultrathin fibers – as thin as a few nanometers – that can be used in preparing membranes with small and defined pore sizes. In addition, due to the small fiber diameter ENMs exhibit high surface area to volume ratio, making them suitable adsorption media with enhanced capacity compared with conventional adsorbents. This paper familiarizes the reader with the history and laboratory-scale preparation of ENMs, discusses parameters that influence properties of the fibers and the final membranes, and introduces a number of applications in which, ENMs have exhibited superior performances compared to competing conventional processes.

Graphical abstract



© 2017 MPRL. All rights reserved.

Contents

1. Introduction.....	229
2. History.....	229
3. Preparation of electrospun nanofiber membranes.....	230
4. Factors affecting properties of ENMs.....	230
4.1. Solution parameters.....	230
4.1.1. Choice of Polymer.....	230
4.1.2. Choice of solvent.....	230
4.1.3. Effect of concentration and viscosity.....	230
4.1.4. Effect of volatility.....	231
4.1.5. Effect of conductivity.....	232
4.2. Operational parameters.....	232
4.2.1. Effect of feed flow rate.....	232
4.2.2. Effect of applied voltage.....	232
4.2.3. Effect of distance from spinneret.....	233

* Corresponding author at: Phone: +1 416 327 3289; fax: +1 416 327 6898
 E-mail address: shahram.tabe@ontario.ca (S. Tabe)

5. Applications.....	234
5.1. Applications in water and wastewater treatment.....	234
5.1.1. Microfiltration.....	234
5.1.2. Ultrafiltration.....	234
5.1.3. Desalination.....	235
5.1.4. Heavy metals removal.....	235
5.1.5. Microorganisms removal.....	235
5.2. Applications in membrane distillation.....	236
5.2.1. Desalination by membrane distillation.....	236
5.2.2. VOCs removal by membrane distillation.....	237
5.2.3. Ethanol/water separation by membrane distillation.....	237
5.3. Air filtration.....	237
6. Summary.....	237
References.....	237

1. Introduction

The recent developments in electrospun nanofiber membranes (ENMs) indicate a breakthrough in the area of separation technology. This is due to a number of unique characteristics that allow for superior performances of ENMs not only compared to the conventional membranes, but also to other competing separation processes. Examples of such characteristics include high porosity, interconnected pores, and high specific surface area. These properties allow for higher fluxes at rejection rates similar to those of conventional membranes with comparable pore sizes. Furthermore, the fiber thickness and the pore size of ENMs can be adjusted through controlling a number of preparation parameters. Because of these properties nanofiber membranes have found potential applications in areas as wide as energy to the environment, water treatment to medicine, and textile to cosmetics.

Technically, the term nanofiber refers to fibers with external dimensions between 1nm and 100 nm [1]. However, in practice, fibers as thick as a few microns are also called nanofibers. Figure 1 shows an SEM image of the surface of a typical nanofiber membrane. As shown, the fibers look like noodles with large and connected void spaces (pores) between them. Different polymeric materials and additives as well as different operating conditions can be used to prepare ENMs with properties suitable for a wide range of applications. Nowadays, nanofibers with diameters in the range of one nanometer to one micrometer can be produced. To better understand how thin a nanofiber could be imagine that more than one million nanofibers could fit in the cross-section of a human hair (assuming diameters of 100 nm and 100 μm for a nanofiber and a human hair, respectively) [2].

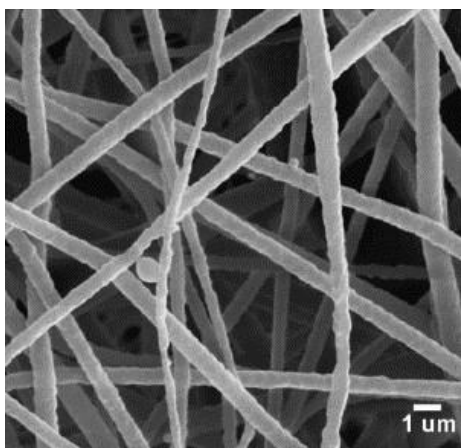


Fig. 1. SEM image of the surface of an electrospun nanofiber membrane (ENM) [5]. The void spaces between the fibers form the interconnected pores allowing flow of fluids through the membrane.

The early applications of ENMs were in air filtration and protective clothing [3,4]. However, the range of pore sizes of ENMs also makes them suitable for other applications such as MF and UF [5] and NF [6]. In addition, because of the large surface area to volume ratio, ENMs have been tested as adsorbents [7]. Furthermore, the high flux of ENMs has opened the door to re-examine membrane distillation [8] as a viable and economical process for a number of applications such as desalination and water/organic separation [9]. For these reasons, ENMs have attracted attention from the industry and academia alike for their more economical and more environmental friendly operation in a number of applications. Figure 2 compares the diameter of

different types of fibers according to their applications [3].

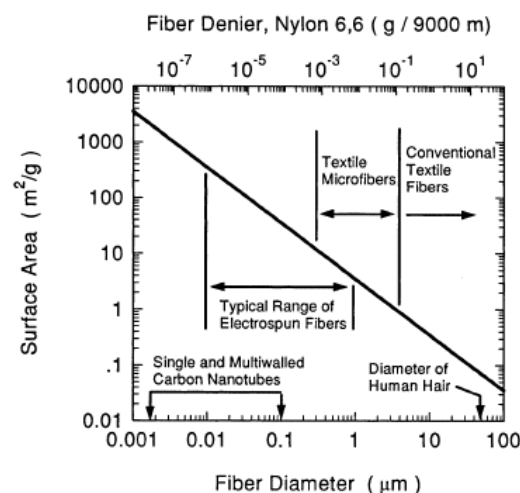


Fig. 2. comparison of diameter and surface area of different fibers according to their applications [3].

2. History

Formation of thin fibers drawn from a solution in an electric field was first tried by Sir Charles Boys [10]. However, the first electrospinning patent was filed by John Cooley in 1902 [11]. The major application of the process was production of “silk-like” threads for textile industry. However, the fibers were quickly entangled and became useless for the purpose. The first breakthrough came with Anton Formhals [12] when he invented an apparatus that produced separate and collectable threads. He used cellulose acetate in a mixture of acetone and alcohol as the spinning solution.

The first use of electrospinning process to produce filters is credited to Nathalie Rozenblum and Igor Petryanov-Sokolov [13]. They produced electrospun fiber mats that were used as filters in gas masks. Like Formhals, they used cellulose acetate as the base material. Despite these works, the progress of electrospinning became slow for a few decades. In early 70s, Baumgarten used the technique to produce fibers with submicron diameters from different concentrations of acrylic resin in dimethyl formamide (DMF). His high-speed photographs show entanglement of the fibers a short distance after they were ejected from a capillary [14]. It was only during the 1990s that electrospun nanofibers started to gain new momentum with the works of the research group at the University of Akron. Darrell Reneker and his group demonstrated production of fine fibers, in the range of few ten nanometers, using a variety of polymeric material [15]. Since then, a large number of research papers have been published on theoretical and technical aspects of electrospun nanofibers and they have found new applications including use in filtration which is the subject of this paper. Figure 3 compares the number of papers published since 1996 until October 2016 on the subject of electrospinning nanofiber membranes.

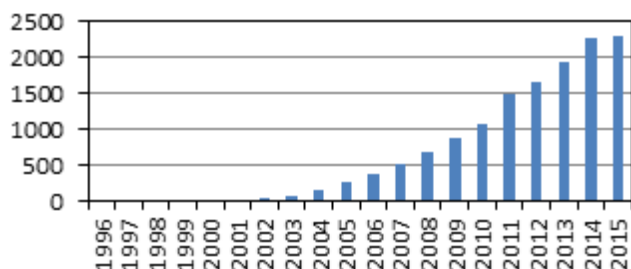


Fig. 3. number of papers published containing keywords “nanofiber OR nanofibre OR nanofibers OR nanofibrous AND electrospinning OR electrospun”. Search made through Scopus, October 2016.

3. Preparation of electrospun nanofiber membranes

In brief, preparation of electrospun nanofiber membranes (ENMs) involves applying high voltage to a polymer solution. The solution ejects as a thin jet that dries and forms a fiber that is collected on a grounded plate. The fibers accumulate on the plate forming a flat sheet that is peeled off and used as membrane.

Conventional spinning techniques such as melt spinning, wet spinning, dry spinning, and gel spinning produce fibers as thin as a few microns in diameter. Thinner fibers – in the range of a few tens to a few hundreds of nanometers – have been produced using other techniques such as template synthesize [16] and self-assembly [17]. The breakthrough, however, came with electrospinning technique which enabled researchers to produce fibers as thin as a few nanometers [15, 18].

The schematic of a simple laboratory set up for preparation of ENMs is shown in Figure 4. The polymer solution is stored in a syringe with a thin needle. An electric voltage, normally in the range of 10,000 to 20,000 volts, is applied between the tip of the needle and a metal ground plate that acts as collector. At high enough voltage, the electrostatic force dominates the surface tension of the polymer solution and a continuous jet ejects from the tip of the needle. The pulling force stretches the stream thinning its size. At the same time, the jet becomes unstable and undergoes bending. The bending increases the distance the polymer solution stream travels before reaching the collector plate. The thinning and longer travel distance together allow for evaporation of the solvent and solidification of the polymer solution in the form of a fiber. The fibers accumulate randomly on the collector plate and form a flat sheet. After the sheet is thick enough it is peeled off the collector plate and used as flat sheet membrane. Post-treatment of the membrane is common.

Suitability of ENMs for certain applications is dictated by characteristics that define the membrane, such as fiber diameter, pore size and pore size distribution, porosity, surface charge, etc. For example, Ma et al. [20] describe a correlation between the fiber diameter and the pore size, such that the pore size is approximately three times the mean fiber diameter. The final properties of ENMs are defined by a number of parameters as will be discussed in the next section.

An extensive presentation of different preparation techniques of ENMs can be found in Feng et al. [19]. Also, Reneker and Yarin [18] provide details of stages of jet and fiber formation and fiber morphology.

4. Factors affecting properties of ENMs

The parameters that dictate the final properties of an ENM are commonly grouped in three categories: solution properties, process properties, and operating conditions [21, 22]. Solution properties include: type of polymer, type of solvent, polymer molecular weight, polymer concentration, solvent viscosity, solvent volatility, surface tension, conductivity, and dielectric constant. Process properties are: needle diameter, applied voltage, distance between the spinneret and the collector, and flow rate. Operating conditions include: temperature, humidity, and composition and flow of the atmosphere.

4.1. Solution parameters

4.1.1. Choice of Polymer

The type of polymer used for preparation of ENMs depends on the final application of membrane. Parameters such as spinnability, surface tension, and hydrophobicity should be considered. Most of the polymers used in conventional membrane preparation can also be used for electrospinning. A

few examples include cellulose acetate (CA), polyvinylidene fluoride (PVDF), polyacrylonitrile (PAN), and polycarbonate (PC).

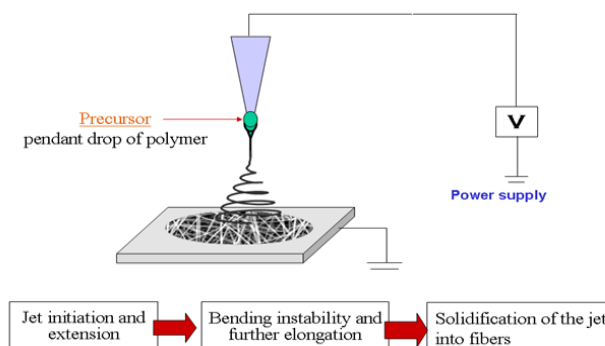


Fig. 4. Schematic of a simple electrospinning set up for nanofiber membrane preparation. Reproduced with permission of [19].

4.1.2. Choice of solvent

Choice of solvent greatly affects spinnability and final properties of the ENMs. Thiagarajan and Sahu [23] studied spinnability nylon-6 in formic acid solutions at different concentrations. They concluded that only at concentrations greater than 16% the solution was spinnable. At the lower end of spinnability, i.e., at 16%, segmental fibers containing beads form. Uniform fibers with no beads formed at concentrations greater than 24%.

A major study on the choice of solvent was done by Jarusuwannapoom et al. [24]. They dissolved polystyrene (PS) in eighteen different solvents at different concentrations and examined the morphological properties of the ENMs by means of scanning electron microscopy (SEM). They found that only five of the solvents produced spinnable solutions. Their qualitative observation suggested that most important factors determining the electrospinnability of the PS solution were high enough values of both the dipole moment of the solvent and the conductivity of both the solvent and the resulting solutions, high enough boiling point of the solvent, not-so-high values of both the viscosity and the surface tension of the resulting solutions. Table 1 compares the SEM images of PS prepared using five different solvents at three concentrations.

Solubility of the polymer and boiling point of the solvent are also two major parameters to consider. Surface tension of the solvent plays an important role in shaping the nanofibers. High surface tension solvents tend to form spheres in order to minimize their surfaces. This, results in formation of droplets instead of fibers or formation of beads in fibers [25]. Therefore, a solvent with lower surface tension is more desirable.

Blending and mixing solvents with desirable characteristics is also common in order to control the properties of the produced fibers and the final membrane. For example, Han et al. [26] used a blend of acetic acid and water at different compositions to dissolve cellulose acetate and observed that the fiber diameter and size distribution are directly affected by the solvent composition. A ternary solvent blend of acetone, DMF, and trifluoroethylene (3:1:1) was also used to dissolve cellulose acetate by Ma et al. [27].

4.1.3. Effect of concentration and viscosity

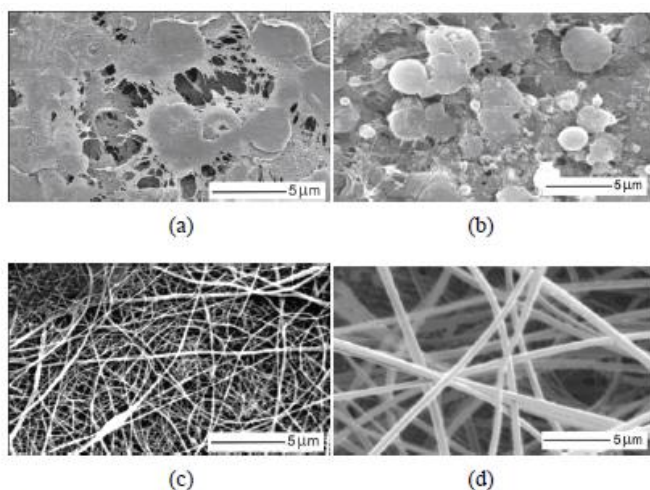
The effects of concentration and viscosity of polymer solution on the morphology of fibers and properties of the produced membranes have been studied by a number of researchers [28-30]. Concentration and viscosity of polymer solution are interconnected to certain extent. Generally, viscosity increases with concentration. A low concentration solution destabilises the ejected jet stream causing breakage of the solution into small droplets. Partial evaporation of the solvent causes the droplets to land as small spheres of polymer. This process is called electrospraying. As the concentration of polymer solution increases the polymer chains interact more and the jet becomes continuous and fibers are formed. That is when electrospinning takes place [15].

The transition between electrospraying and electrospinning has been investigated by Costa et al. [31]. The group prepared two PVDF solutions, one with DMF and the other with DMF/acetone as the solvent. Both solutions were prepared at 5, 7, 10, and 20 wt% concentrations. Figure 5 shows the SEM images of the membranes formed using each of the two solutions and at each of the concentrations.

Table 1

Morphological comparison of polystyrene ENMs prepared using five different solvents at three concentrations [24].

Solution	Solvent				
	1,2-Dichloroethane	DMF	Ethylacetate	MEK	THF
10% w/v					
20% w/v					
30% w/v					

Notes: applied potential: 20 kV, collection distance: 10 cm, scale on the images: 100 μm .**Fig. 5.** SEM images of PVDF in DMF and in DMF/acetone at different concentrations [31].

According to the study, PVDF/DMF solution forms droplets at lower concentrations of 5 and 7 wt%. At 10 wt%, a transition stage was observed where fibers formed, but they contained beads. Only at higher concentration of 20% clean continuous fibers were formed. Comparing the two solutions, the transition happened earlier for PVDF/DMF/acetone system than PVDF/DMF system at a concentration of 7 wt%. Also the fiber thickness increased with increasing concentration for both solutions.

The major differences between the two solutions were in their viscosities and solvent volatilities. In both cases, electrospinning dominated at lower concentrations. However, although acetone is less viscous than DMF, because of its higher volatility it evaporated more rapidly increasing concentration of the jet stream. That, in turn, delayed the destabilization effect and favored continuous jet that allowed for an earlier formation of fibers.

Tungprapa et al. [32] conducted similar study using cellulose acetate in a number of single and binary solvents at varying concentrations. The observations from this group were in agreement with the other studies described here, namely, low concentrations of CA resulted in electrospinning or beaded and short fibers. As the CA concentration increased smooth fibers were produced.

Deitzel et al. [33] used PEO in water solutions to show that there exists an optimum concentration within which fiber diameter increases with concentration according to a power law relationship. The power law relation

was also reported by Demir et al. [34] who used AFM to measure the diameter of fibers obtained from polyurethaneurea in DMF solutions. They observed an increase in fiber diameter from a few nm to ~ 800 nm at concentrations ranging from 3.8 wt% to 12.8 wt%. Similar observations and conclusion were made by Megleski et al. [35] using polystyrene in THF, and by Gu et al. [36] who showed that the diameter of fibers prepared from PAN in DMF increased from ~ 200 nm to $\sim 1,000$ nm when the concentration increased from 6 wt% to 12 wt%.

Molecular weight of the polymer also affects the viscosity, and therefore spinnability of the polymer solution. Molecular weight of a polymer is determined by the length of the polymer chain, which in turn influences the entanglements. Higher molecular weights result in more viscous solutions [37].

In general, an optimum viscosity would be high enough to ensure the jet continuity and low enough for smooth flow of the solution through the needle. For example, Doshi and Reneker [15] determined that the optimum viscosity for PEO/water solutions at different concentrations were between 800 and 4,000 centipoise.

4.1.4. Effect of volatility

Volatility – as determined by boiling point of the solvent – is another determining factor when the final shape and properties of the fibers are concerned [38]. A highly volatile solvent evaporates quickly solidifying the fibers when the jet stream is still too thick. The fibers formed this way would be generally thicker than those formed using a less volatile solvent. On the other hand, a low volatility solvent would not evaporate fast enough for the fibers to solidify and take shape. Fibers land on the plate while still wet, and fuse and form a porous sheet, similar to conventional membranes. A suitable solvent would evaporate at the rate that allows for thinning the jet stream, and at the same time, leaves the jet stream fast enough for the fibers to form before landing on the collection plate.

Volatility of the solvent also affects the surface roughness (porosity) of the nanofibers. This effect was studied by Megleski et al. [35] who electrospun nanofibers from solutions of polystyrene in THF, DMF, and mixtures of the two. They observed that the nanofibers produced from highly volatile THF were porous on the surface, while those from low volatility DMF were smooth. Also, the surface porosity of nanofibers prepared from solutions with different ratios of DMF and THF varied from smooth to rough when the ratio of the solvents varied from favoring DMF to favoring THF.

Similar observations were obtained by Tungprapa et al. [32] when cellulose acetate was dissolved in binary solvent systems. Furthermore, Ma et al. [27] also experimented with ternary blend of solvents to control the morphology of the produced fibers. The group dissolved cellulose acetate in acetone/DMF/trifluoroethanol at 3:1:1 ratio. The produced ENM was then heat treated and used as affinity membrane.

4.1.5. Effect of conductivity

Conductivity of the polymer solution has direct effect on the fiber diameter. A solution with higher conductivity produces finer fibers [8, 39]. That is because higher conductivity means the capacity of a solution for carrying charges is higher and the applied voltage exerts a higher tensile force on a polymer solution with higher conductivity. The tensile force causes more pronounced elongation of the jet stream, thus, formation of finer fibers. The balancing forces on the jet stream include charge repulsion that try to break the stream and surface tension that keeps it together. Therefore, as the applied voltage on the stream increases more elongation of the stream occurs. This means less bead formation and smaller diameter fibers forming. Early studies suggested an inverse relation between the fiber diameter and cubic root of solution conductivity [14].

Conductivity of a polymer solution depends on the choice of solvent as well as on addition of suitable additives to the solution. For example, Nirmala et al. [40] used formic acid as the solvent for polyamide polymer. They observed an increased mass throughput from the spinneret and thinner fibers as the result of increased conductivity of the solution. They explained the improved properties of the fibers by enhanced presence of free ions in the solution.

Several researchers looked at enhancing the conductivity of a solution by adding ionic substances. Ionic salts increase the charge density of the polymer solution. Fong et al. [25] enhanced the conductivity of PEO in water by adding NaCl to the solution. They observed easier ejection of the polymer solution from the nozzle, formation of smaller and smoother fibers, and suppressed beads formation. Zhang et al. [41] added different concentrations of NaCl to polyvinyl alcohol (PVA)/water solution. They observed a decrease in fiber diameter from 214 nm to 159 nm when the salt concentration increased from 0.05% to 0.2%. Zong et al. [42] showed that addition of 1 wt% of three different salts, namely, KH_2PO_4 , NaH_2PO_4 , and NaCl helped elimination of beads that were forming using no-salt solution. The same group also observed that solutions with smaller molecule salts produced thinner fibers. This is due to the larger charge density carried by smaller salts.

Additives other than salts were also used to enhance the conductivity of polymer solution. Son et al. [43] used polyacrylic acid (PAA) and polyallylamine hydrochloride (PAH) as electrolyte additives to a solution of PEO in water. They observed formation of thinner fibers which were attributed to the increased conductivity of the solution.

4.2. Operational parameters

Operational parameters such as feed flow rate, applied voltage, and the distance between the tip of the nozzle and the ground plate, as well as ambient parameters such as temperature, humidity, and atmosphere influence the properties of the fibers and the final membrane.

4.2.1. Effect of feed flow rate

Feed flow rate is an important factor dictating the thickness of the produced fibers. In general, smaller feed flow rates produce thinner fibers. Fridrikh et al. [44] proposed a model predicting the jet diameter as well as the final fiber diameter. The equation defining the limiting diameter of the jet is:

$$h = \left[\left(\frac{2\varepsilon}{\pi(2\ln\chi - 3)} \right) \times \left(\frac{Q^2}{I^2} \right) \times \gamma \right]^{1/3} \quad (1)$$

Where, h represents jet diameter, ε is dielectric permittivity, χ is a dimensionless wavelength of the instability equal to the ratio of radius of curvature to the jet diameter, Q is the feed flow rate, I is electric current, and γ is surface tension. In this equation, the first parenthesis is constant and Q/I is the inverse of volume charge density. The fiber diameter is obtained when the effect of concentration change is incorporated into the above equation:

$$d = c^{1/2} \cdot h \quad (2)$$

Substituting for h and taking logarithm of the two sides results in the following relation:

$$\text{Log } d = 0.667 \log(Q/I) + K \quad (3)$$

where, K is constant. This equation predicts a logarithmic graph of fiber diameter versus Q/I would yield a straight line with a slope of 0.667. Figure 6 compares the experimental results with prediction from the model for polycaprolacton (PCL). The slope of the experimental results is 0.639, in good agreement with the theoretical value. The theoretical curve for jet diameter (insert) was shifted by roughly a constant value of 2, which still is in

good agreement with the theoretical prediction. The difference between the predicted and experimental values could be attributed to the measurements (e.g., of surface tension) as well as to assumptions (e.g., of χ).

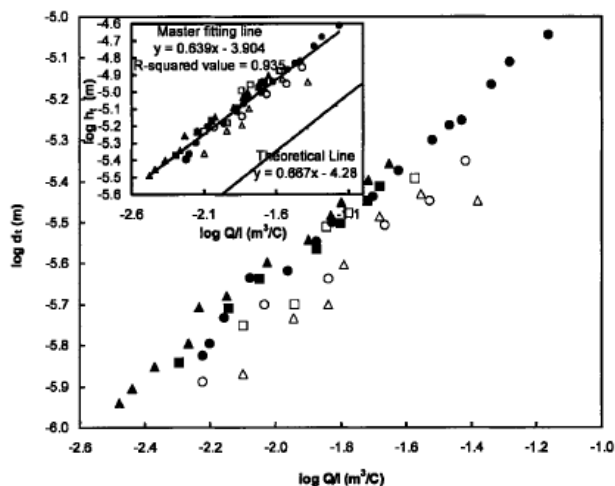


Fig. 6. Log of fiber diameter vs. log of Q/I for polycaprolacton at different concentrations [44].

To examine validity of the model for other systems, the group also tried PEO and PAN, which unlike PCL, have high conductivities. Although they did not succeed to spin solutions of the two polymers to reproducible results over a wide range of Q/I values, the experimental results they obtained fit the predictions within 10% to 20%.

Megelski et al. [35] electrospun polystyrene in THF solution to demonstrate that larger fiber diameters as well as larger pore sizes result from higher flow rates. In addition, a larger amount of solvent needs to evaporate if the flow rate is high. It might cause insufficient drying of the fibers before they reach the collector plate. Wet fibers, as discussed earlier, cause fusion of fibers and formation of flat, ribbon shape fibers. In general, it has been shown that lower flow rates produce smaller fibers and minimizes bead formation [45].

4.2.2. Effect of applied voltage

In the absence of an external force, the surface tension of the polymer solution keeps the molecules together. An electric field charges the surface molecules generating a force opposing the surface tension. At a critical voltage value the electric force overcomes surface tension of the solution and a jet ejects from the tip of the needle. Furthermore, the balance between the two forces induces instability in the jet and causes the jet to bend and whip. The minimum voltage needed to initiate the jet stream depends on the system. For example, a 30% poly lactic acid in DMF required 16 kV before a jet stream is formed [42], while 5.5 kV was already high enough to initiate jet formation in a PEO/water solution at 7 wt% concentration [33].

At low applied voltage, a droplet forms at the bottom of the needle with a cone – known as Taylor cone – hanging from the apex of the drop where the jet starts to eject. As the voltage increases, the droplet becomes smaller until it disappears and the Taylor cone forms at the tip of the needle. Further increase of the voltage would remove the cone and the jet initiates from the inside of the needle. This is shown in Figure 7 [46]. To compensate for the disappearance of Taylor cone, higher flow rate is exercised. Beads formation is also associated with the higher applied voltage.

Dietzel et al. [33] spun PEO in water solutions under varying voltages from 5.5 kV to 15 kV and showed that mass flow rate of the polymer solution is directly related to the applied voltage. They also concluded that intensity of beads increase with increasing the applied voltage. The study suggested that by monitoring the spinning current the formation of beads can be controlled. The correlation between the applied voltage and intensity of bead formation was also reported by Zong et al. [42], Pawlowski et al. [47], and Haghi and Akbari [48].

Both Baumgarten [14] and Sill and von Recum [46] reported that the fiber diameter decreases with increasing applied voltage to certain point and then starts to increase again which coincides with beads formation. The increase in fiber diameter with increasing voltage was also reported by Meechaisue et al. [49]. They explained the increased fiber diameter by larger amounts of polymer solution ejected under the dragging force of the applied

voltage.

Thompson et al. [21] proposed a model that indicated both the transition and the final fiber diameter are affected by the applied voltage. Figure 8 shows that as the applied voltage increases the final radius of the jet decreases. Also, the jet acquires its final size faster.

Nirmala et al. [50] produced polyamide-6 ultrafine fibers at proper applied voltage. The group observed that when the applied voltage reached the critical value of 22 kV ultrafine fibers formed in the shape of a spider web connecting the regular shaped fibers. The diameter of the ultrafine fibers was in the range of 9 to 28 nm, while regular fibers had diameters of 75 to 110 nm (Figure 9). Further increase in the applied voltage caused less ultrafine fibers produced.

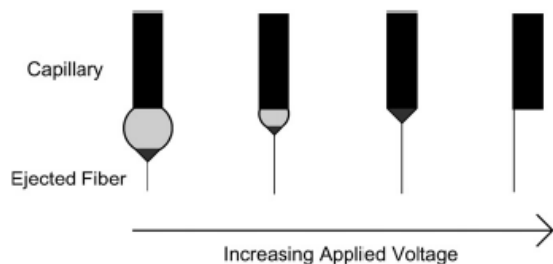


Fig. 7. Effect of varying the applied pressure on the formation of the jet. At relatively low voltages a drop is formed at the tip of the needle with the Taylor cone forming at the apex of the drop where the jet initiates. As the voltage increases the drop disappears and the cone forms at the tip of the needle. Further increase of applied voltage causes the jet to initiate directly from the inside of the needle [46].

4.2.3. Effect of distance from spinneret

The distance between the spinneret and the collector is less profound compared with other parameters. However, it affects the shape and diameter of the fiber by allowing for bending instability and whipping, which in turn, cause both thinning the fibers and evaporation of the solvent. Doshi and Reneker [15] correlated the fiber thickness to the distance between the spinneret and the collector plate and showed that finer fibers were produced when the distance was larger. A short distance means a shorter travel path for the jet, thus, shorter evaporation time. The wet fibers, in such case, would fuse and/or take a flat shape. Megelski [35] observed bead formation when

the distance between the spinneret and the collector was not long enough for elongation and drying of fibers. The distance also plays an important role in switching between electrospaying and electrospinning. The effect of distance from spinneret on fiber diameter is shown in Figure 10 [51].

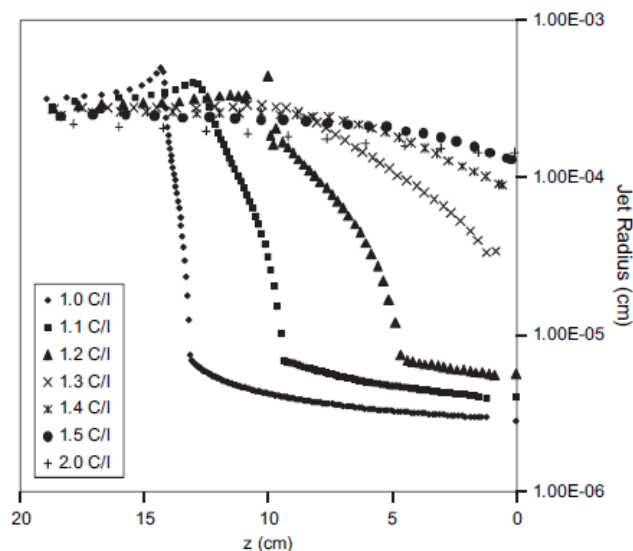


Fig. 8. variation of the jet radius with distance from the ground plate at different applied pressures [21].

An interesting experiment was conducted by Haas et al. [52] where they used a combination of distance between spinneret and collector, mix of solvents with different volatilities, and feed flow rate to obtain fibers with controlled degree of fusion leading to high packing density.

Generally, an optimum distance between the spinneret and the collector is long enough for fiber stretching and solvent evaporation and short enough for preventing breakage of the fiber. Outside this optimum distance bead formation or electrospaying are observed [53].

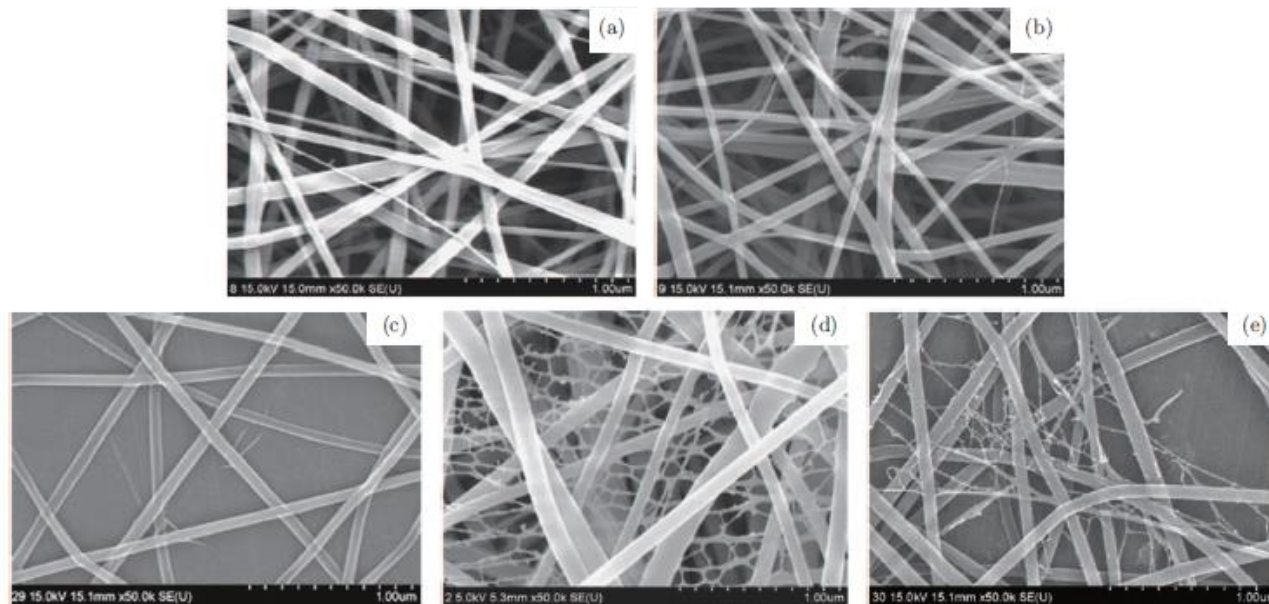


Fig. 9. FE-SEM images of electrospun polyamide-6 produced with different applied voltages of (a) 15, (b) 17, (c) 19, (d) 22, and (e) 25 kV [50].

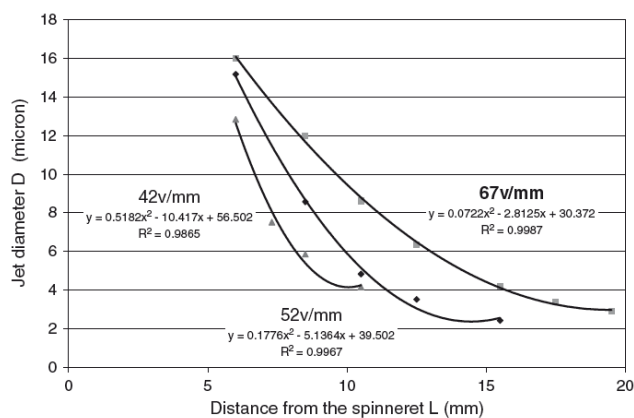


Fig. 10. Decrease of fiber diameter with increasing distance from the spinneret at different applied voltages [51].

5. Applications

The early applications of nanofibers were in textile industry. During the past few decades, however, they have found new applications in filtration, biotechnology, energy, and medical sciences. An investigation of the relevant US patents indicated that medical prosthesis followed by filtration make up the majority of the applications of nanofibers [54]. This is shown in Figure 11.

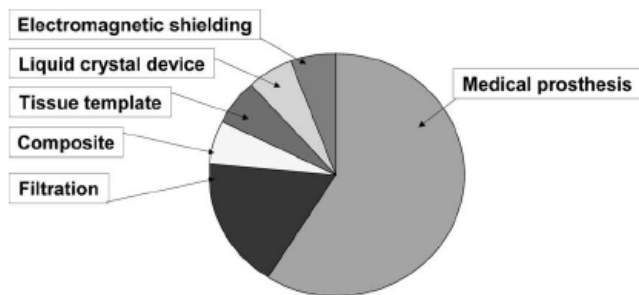


Fig. 11. applications of electrospun nanofibers in different industries according to the US patents [54].

Because this paper is focused on electrospun nanofiber membranes the applications presented here are related to filtration. There are a number of relevant reviews available for medical applications. For example, in dental [37], drug delivery [30, 46], biotechnology [55], antibacterial [56], and cell culture scaffold [40].

The early application of ENMs in the area of filtration was in air cleaning. In the recent years, this new generation of membranes have found applications in other industries such as water and wastewater treatment as well as membrane distillation. The latter was only revived due to the significantly higher flux that ENMs offer compared to conventional membranes. Also, high porosity and high surface area to volume ratio make ENMs suitable for adsorption processes.

5.1. Applications in water and wastewater treatment

During the past decades the market for membrane processes in water and wastewater treatment has shown exponential growth. Novel improvements have enhanced performance and life span of commercial membranes and have significantly reduced cost of treatment. The nanofiber membranes as a new generation of membranes are about to introduce yet another major leap ahead by significantly increase water flux and reducing energy consumption. A number of reviews have focused on the advancements ENMs offer to the water industry [2, 19, 57, 58, 59].

5.1.1. Microfiltration

Microfiltration membranes are commonly used in water and wastewater treatment to remove particulates. They are also used as pre-filter in NF and RO applications. Suitable pore size and high porosity of ENMs make them ideal alternatives for microfiltration applications with superior performances

compared to the conventional membranes [60].

Gopal et al. [61] prepared and characterized electrospun PVDF membranes. The results of the characterization revealed that they have similar properties as conventional MF membranes. The group simulated micro-particle removal using the prepared membranes. For this purpose, they passed polystyrene nanoparticles of nominal size 1, 5, and 10 μm through the prepared ENMs and observed removal efficiencies of between 91% and 98%. As shown in Figure 12, no fouling was observed when 10 μm nanoparticles were used, which was attributed to removal of the particles from the surface of the membrane through good stirring of the feed. As a result, no drop in flux was observed. The experiment with the 5 μm nanoparticles showed some fouling. Nevertheless, the stirring was still sufficient to prevent sever fouling. While the 1 μm particles exhibited the highest removal efficiency, the flux was sharply declined. The SEM image revealed significant deposition of the particles that plugged the pores of the membrane. The pressure-flux correlation indicated that the liquid entry pressure (LEP, the minimum pressure required before a liquid starts to permeate through a membrane) was 7.7 psi. The flux increased exponentially at pressures exceeding the LEP.

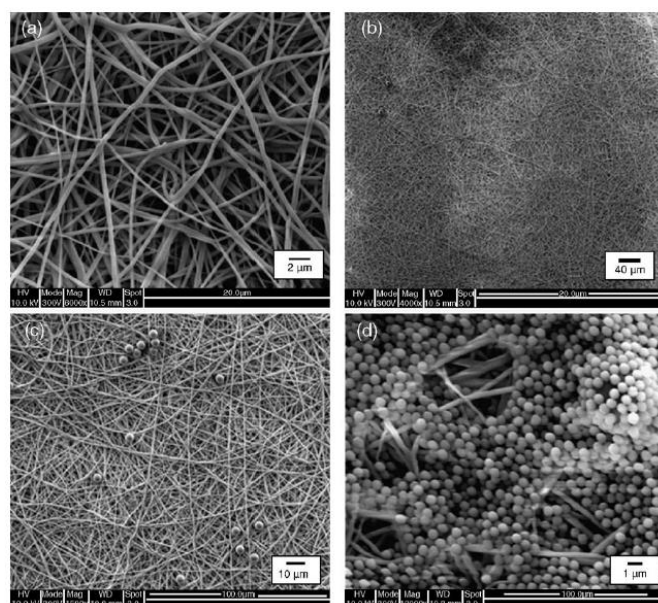


Fig. 12. FESEM images of PVDF ENM: a. before removal, b. after 10 μm removal, c. after 5 μm removal, after 1 μm removal [61].

Gopal et al. [5] also explored use of polysulfone ENM as pre-filter. The group simulated particulate removal in pre-filter applications by using polystyrene nanoparticles from 0.1 μm to 10 μm size. The membrane was able to remove 99+% of 10, 8, and 7 μm particles without any permanent fouling. However it was irreversibly fouled by 2 and 1 μm particles. The membrane was observed to behave as deep filter for particles below 1 μm . the LEP was 2 psi and flux increased exponentially with applied pressure afterwards. The study highlighted the potential of ENMs as a protection barrier for RO and UF applications.

In a similar study, Aussawasathien et al [62] used nylon-6 to remove particulates of sub-micron to 10 μm size. The particles with 1 to 10 μm sizes were removed completely, while those smaller than 1 μm showed rejection efficiency of ~90%. Liu et al. [63] compared performance of a PVA nanofiber membrane crosslinked with glutaraldehyde with that of Millipore GSWP commercial membrane. The PVA ENM exhibited 3 to 7 times higher pure water flux and rejected 98+% of bacteria sized particles.

5.1.2. Ultrafiltration

While the pores of a nanofiber membrane is well fitted with MF applications reducing the size of the pores to the range suitable for ultrafiltration is not straightforward. For this purpose, the concept of thin film nanofibrous composite (TFNC) membrane has been introduced [64]. This configuration adopts the conventional thin film composite (TFC) configuration by incorporating three separate layers into one membrane. The top layer is either a hydrophilic nonporous thin layer or a nanofiber membrane made from ultrafine fibers (in the range of a few nanometers

thick). The middle layer is an ENM containing micropores and the bottom layer is a conventional non-woven support. This configuration is shown in Figure 13.

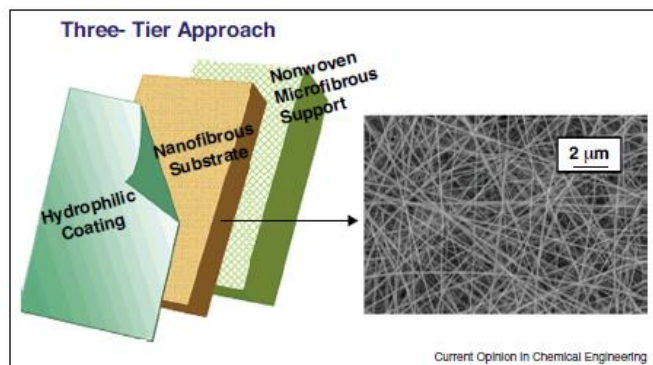


Fig. 13. Schematic diagram of a thin film nanofibrous composite membrane [64].

Yoon et al. [65] demonstrated that UF membranes made of fibers had porosity at least twice as high as conventional UF. Such membranes can remove oil emulsions from water and have applications in oil and gas industries. Ma et al. [20, 66,67,68] replaced the top nonporous layer with a thin layer of ultrafine ENM with fibers having diameters between 5 and 10 nm. The TFNC membranes exhibited 10 times higher flux than commercial membranes.

5.1.3. Desalination

While reverse osmosis desalination has become accepted process worldwide, ENMs offer certain advantages. For example, thin film nanocomposit (TFNC) membranes have offered enhanced flux compared to conventional desalination membranes. This is done by replacing the middle layer of a conventional TFC with a nanofiber membrane. The higher porosity and lower resistance of the middle layer help enhancing the overall flux of the desalination membrane.

Yung et al. [69] prepared a TFNC for nanofiltration by interfacial polymerization of piperazine using ionic liquids. The major characteristic of the TFNC was the use of electrospun PES as support layer of the TFNC which reduced the resistance to the flow of permeating water compared with the conventional UF membranes. The rejection rate of the resulting membrane was examined for $MgSO_4$ and NaCl. The TFNC membrane exhibited 2 times higher permeation flux compared to that of commercial NF-90 with comparable salt rejection ratio, and comparable permeation flux and salt rejection performance as those of NF-270.

5.1.4. Heavy metals removal

Heavy metals need to be removed effectively from drinking water due to their negative effects on human health. For example hexavalent chromium is carcinogenic even at very low dosages, and lead is carcinogenic and causes memory loss if its concentration exceeds limit. Heavy metals enter water sources through the wastewater generated by a number of industries. Kurniawan et al. [70] provide an extensive review of conventional processes for removing heavy metals from wastewater such as chemical precipitation, flotation, membrane filtration, and ion exchange. While these processes are currently in use in large-scale treatment plants they suffer from certain disadvantages such as high cost or low efficiency. Also, in recent years certain agricultural waste and industrial by-products have been used as sorbents to remove heavy metals from wastewater [71]. While the adsorptive capacities of these substances were remarkably high, they introduce CODs, BODs, and TOCs to the water that are major sources of contamination themselves. Removal of heavy metals using the adsorptive properties of ENMs is a novel technique that offers inexpensive and efficient process.

The removal of heavy metals by polymers is based on interactions between the metal and the functional groups on the surface of the polymer. It could be electrostatic interactions, physical affinity, or chemical chelation and complexation [72].

Xiao et al. [73] electrospun blend of polyacrylic acid and polyvinyl alcohol (PAA/PVA) and used it to adsorb copper II ions from water. They succeeded to obtain 91% removal within three hours. Tian et al. [74] electrospun cellulose acetate and surface modified the membrane using

polymethacrylic acid (PMAA) and used to adsorb Cu^{2+} , Hg^{2+} , and Cd^{2+} . The carboxylate group of PMAA significantly enhanced the adsorptive capacity of the base membrane for heavy metals. The best adsorption capacity of the membrane was obtained for mercury at pH=5 which was ~5.3 mg/g. The other two metals showed smaller adsorption capacities of ~2.9 mg/g and ~2.2 mg/g for copper and cadmium, respectively. Irani et al. [75] obtained significantly higher adsorption capacity of 327.3 mg/g for cadmium using polyvinyl alcohol / Tetraethylorthosilicate / aminopyropyltriethoxysilane (PVA/TEOS/APTES) electrospun nanofiber membrane.

Removal of cadmium II, lead II, and copper II from water was also studied by a number of other researchers. Sang et al. [76] used polyvinyl chloride (PVC) for the removal of the target metals. They achieved maximum uptakes of 5.65 mg/g, 5.35 mg/g, and 5.03 mg/g for Cu (II), Cd (II), and Pb (II), respectively. Higher adsorption capacities of the same target heavy metals were obtained using polyethyleneimine ENM by Wang et al. [77]. The membrane was crosslinked, doped with PVA as fiber forming additive, and used as chelating agent to remove the targeted heavy metals. The removal efficiency was the best for Cu (II) with 1.05 mmol/g (67.16 mg/g) followed by Cd (II) with 1.04 mmol/g (116.94 mg/g), and Pb (II) with 0.43 mmol/g (90.03 mg/g). Aliabadi et al. [78] reported adsorption of nickel, copper, cadmium, and lead using ENMs made of PEO/chitosan. The adsorption capacity of the membrane after two hours was 175.1 mg/g for nickel, 163.7 mg/g for copper, 143.8 mg/g for cadmium, and 135.4 mg/g for lead.

Removal of chromium VI was studied by Taha et al. [79]. Chromium VI was removed using amine-functionalized cellulose acetate/silica composite nanofiber membrane. Amine groups can bind with a number of metals. An adsorption capacity of 19.46 mg/g was obtained after 60 min. However, the process required an acidic ambience of pH = 1.0. Li et al. [80] examined Cr VI removal and conversion to Cr III using a composite membrane made of polyamide 6 and Fe_3O_4 . They achieved a removal rate of 150 mg/g. Amine-functionalization was also applied to PAN by Kampalanonwat and Supaphol [81] for removing Cu (II), Ag (II), Fe (II), and Pb (II). The experimental results fitted well with Langmuir isotherm as shown in Figure 14.

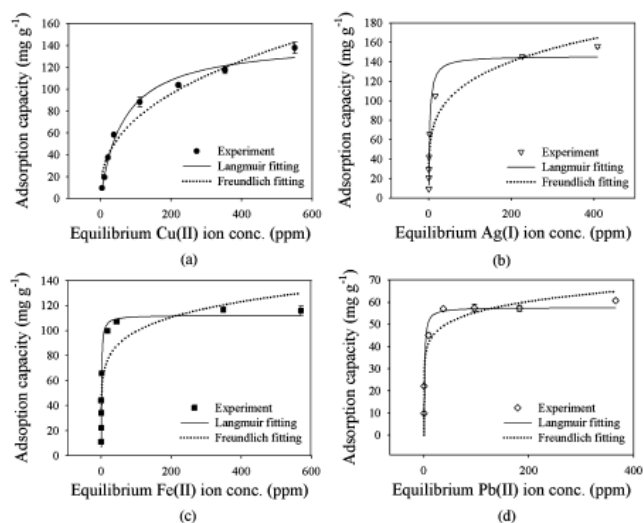


Fig. 14. Adsorption isotherms of Cu (II), Ag (II), Fe (II), and Pb (II) onto amino-functionalized PAN membrane [81].

Chromium III removal was examined by Taha et al. [82] using an amine-functionalized polyvinyl pyrrolidone (PVP)/ SiO_2 . An adsorption capacity of 97 mg/g was obtained at pH=7.5. The adsorption equilibrium was achieved after 20 min. The adsorption capacity reduced from 97% to 92% after five cycles of regeneration.

Thioether-functionalized polyvinyl pyrrolidone (PVP)/ SiO_2 was used by Teng et al. [83] to remove Hg^{2+} from water. At an optimum condition they achieved 4.26 mmol/g (~855 mg/g) adsorption capacity. The equilibrium was achieved after 30 min and the adsorption capacity remained the same after three regeneration cycles.

5.1.5. Microorganisms removal

Removal and/or deactivation of microorganisms using ENMs are possible by size exclusion or by adsorption. ENMs with definite pore sizes

have been developed that reject microorganisms of specific sizes. Also, a variety of antibacterial agents such as zinc oxide, titanium dioxide, and silver have been incorporated into membranes for this purpose. Different approaches exist for incorporation of active agent into the fibers. The active agent can be blended with the polymer solution prior to electrospinning, be confined in the core of the fiber through coaxial electrospinning, be encapsulated in nanostructures before dispersing them in the solution, or through post-treatment to convert precursor into its active form, or by attaching onto the surface of the fiber [56]. These approaches are schematically shown in Figure 15.

Zhang et al. [84] treated PAN ENM in hydroxylamine aqueous solution to produce amidoxime nanofiber membrane. The active $-C(NH_2)=N-OH$ group on the surface of the fibers were used to coordinate Ag^+ , which were then converted to Ag nanoparticles. The efficiency of the produced ENMs was tested against deactivation of *S. aureus* and *E. coli*. The membranes with Ag^+ and with Ag nanoparticles both were capable of 7 log removal after 30 min of contact time.

5.2. Applications in membrane distillation

Although membrane distillation (MD) processes have been proven viable from technical point of view, they haven't experienced economic growth mainly due to their low fluxes. The development of nanofiber membranes have brought attentions back to MD because of the high flux that these membranes offer. A number of research groups have focused on incorporation of ENMs into MD processes for applications such as water and wastewater treatment as well as desalination.

Membrane distillation is a thermally driven process that works according to the vapor pressure difference across a membrane. The feed, at temperatures below its boiling point, flows on one side of a hydrophobic membrane. Water vapor enters the pores of the membrane, is transport to the other side, which is at a lower temperature, condenses, and is collected. Table 2 [8] shows the schematics of different membrane distillation configurations. Camacho et al. [85] have published a comprehensive review on the applications of membrane distillation in desalination. Also, Khayet and Matsuura [86] provide a history of membrane distillation.

5.2.1. Desalination by membrane distillation

The first attempt to use ENMs in MD was made by Feng et al. [9] to produce drinking water ($NaCl < 280$ ppm) from saline water solutions of 1%, 3.5%, and 6% concentrations. They tested the membrane at different temperature differences ranging from 15 °C to 60 °C. Flux increased with increasing temperature and decreasing salt content of the feed. Flux of 1% NaCl ranged from ~ 1.5 kg/m² h at $\Delta T = 15$ °C to a maximum of ~ 11.5 kg/m² h at $\Delta T = 60$ °C. Salt rejection was high at all experimental conditions and ranged from 98.5% to 99.9%. During an experimental period of 25 days stable results were obtained. Figure 16 shows the variations in flux and salt rejection with temperature difference across the membrane.

The same group experimented with embedding clay nanoparticles in PVDF polymer to enhance hydrophobicity [87]. They used the produced ENM for direct contact membrane distillation (DCMD) and achieved 99.97%

salt rejection at a flux of ~ 5.7 kg/m² h.

In a similar experiment, the group added hydrophobic surface modifying macromolecules (SMM) and pore forming polyvinyl pyrrolidone to PVDF and used the produced ENM for desalting 3.5% salt water [88]. They obtained $\sim 99.98\%$ salt rejection at fluxes up to 20 kg/m²h.

Zhang et al. [89] compared the performance of commercial microfiltration PVDF membrane with four different commercial microfiltration PTFE membranes for membrane distillation desalination. The porosities of the active layers of the membranes were between 81.0% and 92.9%. They concluded that the performances of the membranes made of PTFE were superior to PVDF with a salt rejection rate of nearly 100% against 96%. The best flux obtained using PTFE membranes were ~ 25 L/m² h compared with ~ 20 L/m² h for PVDF.

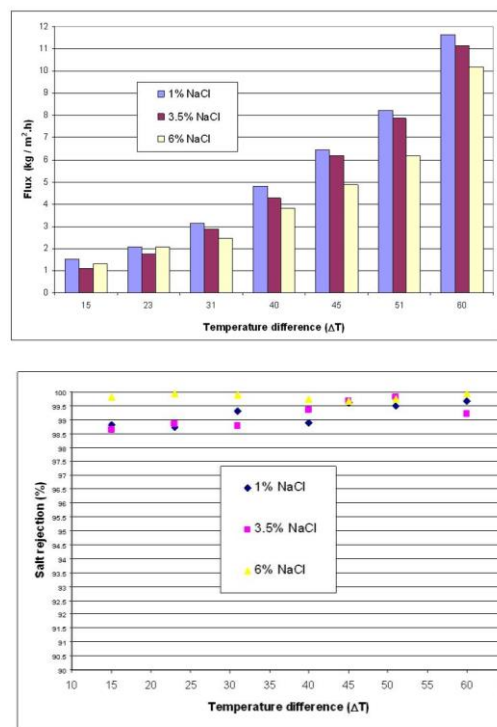


Fig. 16. Variations of flux and salt rejection with temperature difference across the membrane [9].

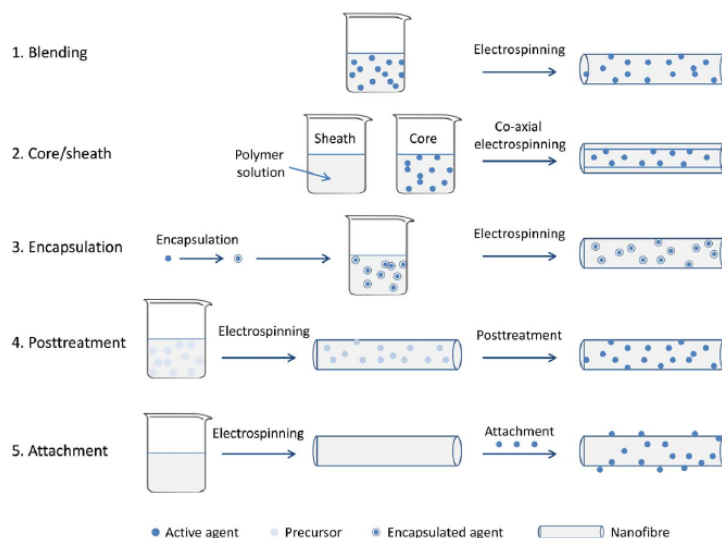
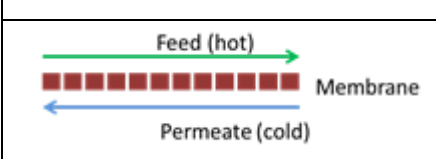
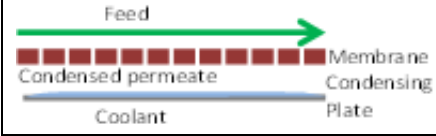
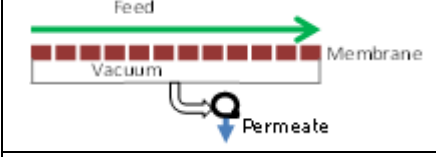
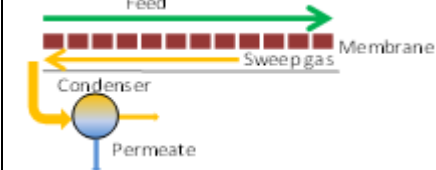


Fig. 15. Various methods of incorporating antibacterial agents into nanofiber membranes [56].

Table 2
Different configurations of membrane distillation.

	Configuration	Remarks
	Direct contact membrane distillation (DCMD)	<ul style="list-style-type: none"> Feed flows on one side of the membrane, permeates through pores in vapor form and condenses on the other side. Both feed and permeate are in direct contact with membrane.
	Air gap membrane distillation (AGMD)	<ul style="list-style-type: none"> Feed flows on one side of the membrane. The permeate condenses on a cooled plate separated from the membrane by an air gap.
	Vacuum membrane distillation (VMD)	<ul style="list-style-type: none"> Feed flows on one side of the membrane. Permeate is collected under vacuum and is condensed outside the membrane cell.
	Sweep Gas Membrane Distillation (SGMD)	<ul style="list-style-type: none"> Feed flows on one side of the membrane. A gas flows on the other side collecting the permeate vapor. The stream then goes through a condenser where the permeate is collected in liquid form.

5.2.2. VOCs removal by membrane distillation

ENMs were used as both filters and adsorbents to remove VOCs from water or wastewater. Singh et al. [7] carbonized PAN ENM by heating the membrane under nitrogen atmosphere at 400 °C for 4 hours. The carbonized membrane was used to remove chloroform and monochloroacetic acid from water. Adsorption capacities of 554 mg/g and 504 mg/g were obtained for chloroform and monochloroacetic acid, respectively.

Feng et al. [90] used gas stripping membrane distillation (GSMD) to remove chloroform as a typical VOC from water. Nitrogen was used as the sweep gas. The feed concentration varied from 250 to 2,000 ppm. The feed temperature was from 23 to 60 °C. They observed a fast depletion of the feed from chloroform such that in 5 hours between 60% and 85% of chloroform was removed from water depending on the feed concentration.

5.2.3. Ethanol/water separation by membrane distillation

Formation of azeotropic mixtures of ethanol and water makes separation of the two difficult. Feng et al. [19] report ethanol/water separation using vacuum membrane distillation using PVDF ENM. The feed concentration varied between 20% and 80% ethanol. The corresponding permeate concentrations were between 38 and 85% corresponding to selectivities of 1.4 to 2.4. Flux increased with increasing ethanol concentration in the feed and with increasing temperature. The range of flux was between 1.5 kg/m² h and 3.3 kg/m² h.

5.3. Air filtration

Air filtration requires low flow resistance, low pressure drop, and high flux across the membrane, which all can be found in ENMs. Due to their smaller fiber diameter and larger surface area per volume, ENMs perform superior to conventional air filters [91]. Most common processes where ENMs can be used as air filter media include internal combustion engines, clean rooms for electronic applications, hospitals, and indoor spaces.

Ahn et al. [92] compared the efficiency of a Nylon-6 ENM with that of commercial air filters. Nylon-6 performed better with 99.99% removal efficiency with challenge particles of 0.3 μm in diameter.

The benefits of ENMs in air filtration have been shown by Podgórski et al. [93] who demonstrated nanofiberous media as reliable and inexpensive process to filter most aerosol particles. Their recommended configuration includes a three-layer filter. The top layer is a coarse filter to remove relatively large particles of micron range size. The middle layer is a nanofiberous mat for removal of fine aerosol particulates, with a packed support layer at the bottom.

The composite configuration was also used by Kim et al. [94] and Wang et al. [95]. Both groups used a commercial microfibrinous non-woven filter and

coated them with nanofiber membranes. The former group used PAN nanofiber membrane as the top layer and the latter one used PA-66. Both groups reported significantly enhanced (up to 99.9%) aerosol removal efficiency.

6. Summary

The science and engineering of electrospinning nanofiber membranes (ENMs) have advanced rapidly in the recent years. Fibers with smaller diameters have been produced leading to membranes with smaller and more defined pore sizes. Many successful attempts to modify the chemistry and surface properties of ENMs have resulted in more robust membranes with favorable performances.

ENMs have proven reliable as both filters and adsorbents. As filters, ENMs have found applications in water and wastewater treatment, desalination, air cleaning, as well as food, pharmaceutical, and oil and gas industries. As adsorbents, ENMs offer high surface area to volume ratio and perform superior to conventional adsorption processes in a number of applications. Removal of heavy metals from wastewater is an example of applications where ENMs can be used as adsorption media.

With rapidly growing knowledge and reliable lab-scale and industrial results obtaining using ENMs in different areas it is expected to see these membranes replace a number of conventional processes offering more environmentally friendly and less expensive performances.

References

- [1] ISO/TS 80004-2:2015, http://www.iso.org/iso/home/store/catalogue_ics/catalogue_detail_ics.htm?csnumber=54440, last visited October 2016.
- [2] S. Tabe, Electrospun nanofiber membranes and their applications in water and wastewater treatment, in: Anming Hu and Allen Appleby (Eds.), *Nanotechnology for Water Treatment and Purification*, Springer, Switzerland, 2014, pp. 111-143.
- [3] P. Gibson, H. Schreuder-Gibson, D. Rivin, Transport properties of porous membranes based on electrospun nanofibers, *Colloids and Surfaces* 187-188 (2001) 469-481
- [4] H.Schreuder-Gibson, P. Gibson, K. Senecal, M. Sennett, J. Walker, W. Yeomans, D. Ziegler, and P.P. Tsai, Protective textile materials based on electrospun nanofibers, *J. Adv. Mat.* 34 (2002) 44-55.
- [5] R. Gopal, S. Kaur, C.Y. Feng, C. Chan, S. Ramakrishna, S. Tabe, T. Matsuura, Electrospun nanofibrous polysulfone membranes as pre-filters: Particulate removal, *J. Membr. Sci.* 289 (2007) 210-219.
- [6] S. Kaur, S. Sundarajan, R. Gopal, S. Ramakrishna, Formation and characterization of polyamide composite electrospun nanofibrous membranes for salt separation, *J. Appl. Polym. Sci.* 124 (2012) 205-215.
- [7] G. Singh, D. Rana, T. Matsuura, S. Ramakrishna, R.M. Narbaitz, S. Tabe,

- Removal of disinfection byproducts from water by carbonized electrospun nanofibrous membranes, *Sep. Purif. Technol.* 74 (2010) 202-212.
- [8] L.D. Tijing, J. Choi, S. Lee, S. Kim, H.K. Shon, Recent progress of membrane distillation using electrospun nanofibrous membrane, *J. Membr. Sci.* 453 (2014) 435-462.
- [9] C. Feng, K.C. Khulbe, T. Matsuura, R. Gopal, S. Kaur, S. Ramakrishna, M. Khayet, Production of drinking water from saline water by air-gap membrane distillation using polyvinylidene fluoride nanofiber membrane, *J. Membr. Sci.* 311 (2008) 1-6.
- [10] C.V. Boys, On the Production, Properties, and some suggested Uses of the Finest threads, *Proceedings of the Physical Society* 9 (1887) 8-19.
- [11] J. F. Cooley, Apparatus for electrically dispersing fluids, U.S. Patent 692,631, 1902.
- [12] A. Formhals, Process and apparatus for preparing artificial threads, US Patent 1,975,504, 1934.
- [13] Izvestiya, On the 100th anniversary of the birth of I.V. Petryanov-Sokolov, *Izvestiya, Atmosph. Ocean. Phys.* 43 (2007) 395-395.
- [14] P.K. Baumgarten, Electrostatic Spinning of Acrylic Microfibers, *J. Colloid Interface Sci.* 36 (1971) 71-79.
- [15] J. Doshi, D.H. Reneker, Electrospinning process and applications of electrospun fibers, *J. Electrostatics*, 35 (1995) 151-160.
- [16] V.M. Cepak, J.C. Hulteen, G. Che, K.B. Jirage, B.B. Lakshmi, E.R. Fisher, C.R. Martin, Chemical strategies for template syntheses of composite micro- and nanostructures, *Chem. Mater.* 9 (1997) 1065-1067.
- [17] N.I. Kovtyukhova, B.R. Martin, J.K.N. Mbindyo, T.E. Mallouk, M. Cabassi, T.S. Mayer, Layer-by-layer self-assembly strategy for template synthesis of nanoscale devices, *Mater. Sci. Eng. C* 19 (2002) 255-262.
- [18] D.H. Reneker and A.L. Yarin, Electrospinning jets and polymer nanofibers, *Polymer* 49 (2008) 2387-2425.
- [19] C. Feng, K.C. Khulbe, T. Matsuura, S. Tabe, A.F. Ismail, Preparation and characterization of electrospun nanofiber membranes and their possible applications in water treatment, *J. Sep. Purif.* 102 (2013) 118-135.
- [20] H. Ma, C. Burger, B.S. Hsiao, B. Chu, Ultra-fine cellulose nanofibers: new nanoscale materials for water purification, *J. Mater. Chem.* 21 (2011) 7507-7510.
- [21] C.J. Thompson, G.G. Chase, A.L. Yarin, D.H. Reneker, Effects of parameters on nanofiber diameter determined from electrospinning model, *Polymer* 48 (2007) 6913-6922.
- [22] J. Stranger, N. Tucker, M. Staiger, Electrospinning, *Smithers Rapra*, Shrewsbury, Shropshire, GBR, 2009.
- [23] R. Thiyagarajan and O. Sahu, Preparation and characterization of polymer nanofibers produced from electrospinning, *J. Optoelectronic Eng.* 2 (2014) 24-28.
- [24] T. Jarusuwanapoom, W. Hongrojanawiwat, S. Jitjaicham, L. Wannatong, M. Nithitanakul, C. Pattamaprom, P. Koombhongse, R. Rangkupan, P. Supaphol, Effect of solvents on electro-spinnability of polystyrene solutions and morphological appearance of resulting electrospun polystyrene fibers, *Europ. Polym. J.* 41 (2005) 409 - 421.
- [25] H. Fong, I. Chun, D.H. Reneker, Beaded nanofibers formed during electrospinning, *Polymer* 40 (1999) 4585-4592.
- [26] S.O. Han, J.H. Youk, K.D. Min, Y.O. Kang, W.H. Park, Electrospinning of cellulose acetate nanofibers using a mixed solvent of acetic acid/water: Effects of solvent composition on the fiber diameter, *Mater. Lett.* 62 (2008) 759-762.
- [27] Z. Ma, M. Kotaki, S. Ramakrishna, Electrospun cellulose nanofiber as affinity membrane, *J. Membr. Sci.* 265 (2005) 115-123.
- [28] J. Venugopal, Y.Z. Zhang, S. Ramakrishna, Electrospun nanofibers: biomedical applications, *Proc. the Institution of Mech. Eng. N* 218 (2005) 35-45.
- [29] A. Greiner and J.H. Wendorff, Electrospinning: a fascinating method for the preparation of ultrathin fibers, *Angewandte Chemie* 46 (2007) 5670-5703.
- [30] V. Pillay, C. Dott, Y.E. Choonara, C. Tyagi, L. Tomar, A Review of the Effect of Processing Variables on the Fabrication of Electrospun Nanofibers for Drug Delivery Applications, *J. Nanomaterials*, Article ID 789289, 22 pages, 2013.
- [31] L.M.M. Costa, R.E.S. Bretas, R. Gregorio Jr., Effect of Solution Concentration on the Electrospun/Electrospinning Transition and on the Crystalline Phase of PVDF, *Materials Sci. App.* 1 (2010) 247-252.
- [32] S. Tungprapa, T. Puangparn, M. Weerasombut, I. Jangchud, P. Fakum, S. Semongkhon, C. Meechaisue, P. Supaphol, Electrospun cellulose acetate fibers: effect of solvent system on morphology and fiber diameter, *Cellulose* 14 (2007) 563-575.
- [33] J.M. Deitzel, J. Kleinmeyer, D. Harris, N.C. Beck Tan, The effect of processing variables on the morphology of electrospun nanofibers and textiles, *Polymer* 42 (2001) 261-272.
- [34] M.M. Demir, I. Yilgor, E. Yilgor, B. Erman, Electrospinning of Polyurethane Fibers, *Polymer* 43 (2002) 3303-3309.
- [35] S. Megelski, J. S. Stephens, D. Bruce Chase, and J. F. Rabolt, Micro- and nanostructured surface morphology on electrospun polymer fibers, *Macromolecules* 35 (2002) 8456-8466.
- [36] S.Y. Gu, J. Ren, G.J. Vancso, Process optimization and empirical modeling for electrospun polyacrylonitrile (PAN) nanofiber, *Europ. Polym. J.* 41(2005) 2559-2568.
- [37] M. Zafar, S. Najeeb, Z. Khurshid, M. Vazirzadeh, S. Zohaib, B. Najeeb, F. Sefat, Potential of Electrospun Nanofibers for Biomedical and Dental Applications, *Materials* 9 (2016) 73.
- [38] J. Lannutti, D. Reneker, T. Ma, D. Tomasko, D. Farson, Electrospinning for tissue engineering scaffolds, *Mater. Sci. Eng. C* 27 (2007) 504-509.
- [39] L. Huang, K. Nagapudi, R.P. Apkarian, E.L. Chaikof, Engineered collagen-PEO nanofibers and fabrics, *J. Biomater. Sci. Polym. Ed.* 12 (2001) 979-993.
- [40] R. Nirmala, R. Navamathavan, S. Park, H.Y. Kim, Recent Progress on the Fabrication of Ultrafine Polyamide-6 Based Nanofibers Via Electrospinning: A Topical Review, *Nano-Micro Lett.* 6 (2014) 89-107.
- [41] C.X. Zhang, X.Y. Yuan, L.L. Wu, Y. Han, J. Sheng, Study on morphology of electrospun poly(vinyl alcohol) mats, *Eur. Polym. J.* 41 (2005) 423-432.
- [42] X. Zong, K. Kim, D. Fang, S. Ran, B.S. Hsiao, B. Chu, Structure and process relationship of electrospun bioabsorbable nanofiber membranes, *Polymer* 43 (2002) 4403-4412.
- [43] W.K. Son, J.H. Youk, T.S. Lee, W.H. Park, The effects of solution properties and polyelectrolyte on electrospinning of ultrafine poly(ethylene oxide) fibers, *Polymer* 45 (2004) 2959-2966.
- [44] S.V. Fridrikh, J.H. Yu, M.P. Brenner, G.C. Rutledge, Controlling the Fiber Diameter during Electrospinning, *Phys. Rev. Lett.* 90 (2003) 144502-1 - 144502-4.
- [45] K. Garg, G.L. Bowlin, Electrospinning jets and nanofibrous structures, *Biomicrofluidics* 5 (2011) 013403-1 - 013403-19.
- [46] T.J. Sill and H. A. von Recum, Electrospinning: applications in drug delivery and tissue engineering, *Biomaterials* 29 (2008) 1989-2006.
- [47] K.J. Pawlowski, C.P. Barnes, E.D. Boland, G.E. Wnek, G.L. Bowlin, Biomedical nanoscience: electrospinning basic concepts, applications, and classroom demonstration, *Materials Research Society Symposium Proceedings* 827 (2004) 17-28.
- [48] A.K. Haghi and M. Akbari, Trends in electrospinning of natural nanofibers, *Physica Status Solidi (A) Applications and Materials* 204 (2007) 1830-1834.
- [49] C. Meechaisue, R. Dubin, P. Supaphol, V. P. Hoven, and J. Kohn, Electrospun mat of tyrosine-derived polycarbonate fibers for potential use as tissue scaffolding material, *J. Biomater. Sci.* 17 (2006) 1039-1056.
- [50] R. Nirmala, K.T. Nam, S.J. Park, Y.S. Shin, R. Navamathavan, H.Y. Kim, Formation of high aspect ratio polyamide-6 nanofibers via electrically induced double layer during electrospinning, *Appl. Surf. Sci.* 256 (2010) 6318-6323.
- [51] H. Xu, A.L. Yarin, D.H. Reneker, Characterization of fluid flow in jets during electrospinning, *Polymer* 44 (2003) 51-52.
- [52] D. Haas, S. Heinrich, P. Greil, Solvent control of cellulose acetate nanofiber felt structure produced by electrospinning, *J. Mater. Sci.* 45 (2010) 1299-306.
- [53] N. Bhardwaj and S.C. Kundu, Electrospinning: a fascinating fiber fabrication technique, *BioTechnol. Adv.* 28 (2010) 325-347.
- [54] Z.-M. Huang, Y.-Z. Zhang, M. Kotaki, S. Ramakrishna, A review on polymer nanofibers by electrospinning and their applications in nanocomposites, *Compos. Sci. Technol.* 63 (2003) 2223-2253.
- [55] R. Konwarh, N. Karak, M. Misra, Electrospun cellulose acetate nanofibers: The present status and gamut of biotechnological applications, *BioTechnol. Adv.* 31 (2013) 421-437.
- [56] Y. Gao, Y.B. Truong, Y. Zhu, I.L. Kyratzis, Electrospun Antibacterial Nanofibers: Production, Activity, and In Vivo Applications, *J. Appl. Polym. Sci.* 131 (2014).
- [57] M.I. Litter, W. Choi, D.D. Dionysiou, P. Falaras, A. Hiskia, G.L. Puma, T. Pradeep, J. Zhao, Nanotechnologies for the treatment of water, air and soil, *J. Hazard. Mater.* 211-212 (2012) 1-2.
- [58] S.A.A.N. Nasreen, S. Sundarajan, S.A.S. Nizar, R. Balamurugan, S. Ramakrishna, Advancement in electrospun nanofibrous membranes modifications and their applications in water treatment, *Membranes* 3 (2013) 266-284.
- [59] X. Qu, P.J.J. Alvarez, Q. Li, Applications of nanotechnology in water and wastewater treatment, *Water Res.*, 47, 12 (2013) 3931-3946.
- [60] R. Barhate, C.K. Loong, S. Ramakrishna, Preparation and characterization of nanofibrous filtering media, *J. Membr. Sci.* 283 (2006) 209-218.
- [61] R. Gopal, S. Kaur, Z. Ma, C. Chan, S. Ramakrishna, T. Matsuura, Electrospun nanofibrous filtration membrane, *J. Membr. Sci.* 281 (2006) 581-586.
- [62] D. Aussawasathien, C. Teerawattananon, A. Vongachariya, Separation of micron to sub-micron particles from water: electrospun nylon-6 nanofiber membranes as pre-filters, *J. Membr. Sci.* 315 (2008) 11-19.
- [63] Y. Liu, R. Wang, H. Ma, B.S. Hsiao, B. Chu, High-flux microfiltration filters based on electrospun polyvinylalcohol nanofiber membranes, *Polymer* 54 (2013) 548-556.
- [64] X. Wang, X. Chen, K. Yoon, D. Fang, B.S. Hsiao, B. Chu, High flux filtration medium based on nanofibrous substrate with hydrophilic nanocomposite coating, *Environ. Sci. Technol.* 39 (2005) 7684-7691.
- [65] K. Yoon, K. Kim, X. Wang, D. Fang, B.S. Hsiao, B. Chu, High flux ultra-filtration membranes based on electrospun nanofibrous PAN scaffolds and chitosan coating, *Polymer* 47 (2006) 2434-2441.
- [66] H. Ma, C. Burger, B.S. Hsiao, B. Chu, Ultrafine polysaccharide nanofibrous membranes for water purification, *Biomacromolecules* 12 (2011) 970-976.
- [67] H. Ma, B.S. Hsiao, B. Chu, Thin-film nanofibrous composite membranes containing cellulose or chitin barrier layers fabricated by ionic liquids, *Polymer* 52 (2011) 2594-2599.
- [68] H.Y. Ma, C. Burger, B.S. Hsiao, B. Chu, Fabrication and characterization of cellulose nanofiber based thin-film nanofibrous composite membranes, *J. Membr. Sci.* 454 (2014) 272-282.
- [69] L. Yung, H. Ma, X. Wang, K. Yoon, R. Wang, B.S. Hsiao, B. Chu, Fabrication of thin-film nanofibrous composite membranes by interfacial polymerization using ionic liquids as additives, *J. Membr. Sci.* 365 (2010) 52-58.
- [70] T.A. Kurniawan, G. Chan, W.H. Lo, S. Babel, Physico-chemical treatment techniques for wastewater laden with heavy metals, *Chem. Eng. J.* 118 (2006) 83-98.
- [71] Y. Huang, Y.-E. Miao, T. Liu, Electrospun Fibrous Membranes for Efficient Heavy Metal Removal, *J. Appl. Polym. Sci.*, 131 (2014).
- [72] B.L. Rivas, N. Maureira, C. Guzmán, Water-soluble polymers and their polymer-metal ion-complexes as antibacterial agents, *Macromol. Symp.* 287 (2010) 69-79.
- [73] S.L. Xiao, M. Shen, H. Ma, R. Guo, M. Zhu, S. Wang, X. Shi, Fabrication of Water-Stable Electrospun Polyacrylic Acid-Based Nanofibrous Mats for Removal of Copper (II) Ions in Aqueous Solution, *J. App. Polym. Sci.* 116

- (2010) 2409–2417.
- [74] Y. Tian, M. Wu, R. Liu, Y. Li, D. Wang, J. Tan, R. Wu, Y. Huang, Electrospun membrane of cellulose acetate for heavy metal ion adsorption in water treatment, *Carbohydr. Polym.* 83 (2011) 743–748.
- [75] M. Irani, A.R. Keshtkar, M.A. Moosavian, Removal of cadmium from aqueous solution using mesoporous PVA/TEOS/APTES composite nanofiber prepared by sol-gel/electrospinning, *Chem. Eng. J.* 200–202 (2010) 192–201.
- [76] Y. Sang, F. Li, Q. Gu, C. Liang, J. Chen, Heavy metal-contaminated groundwater treatment by a novel nanofiber membrane, *Desalination* 223 (2008) 349–360.
- [77] X. Wang, M. Min, Z. Liu, Y. Yang, Z. Zhou, M. Zhu, Y. Chen, B.S. Hsiao, Poly(ethyleneimine) nanofibrous affinity membrane fabricated via one step wet-electrospinning from poly(vinyl alcohol)-doped poly(ethyleneimine) solution system and its application, *J. Membr. Sci.* 379 (2011) 191–199.
- [78] M. Aliabadi, M. Irani, J. Ismaeili, H. Piri, M.J. Parmian, Electrospun nanofiber membrane of PEO/Chitosan for the adsorption of nickel, cadmium, lead and copper ions from aqueous solution, *Chem. Eng. J.* 220 (2013) 237–243.
- [79] A.A. Taha, Y. Wu, H. Wang, F. Li, Preparation and application of functionalized cellulose acetate/silica composite nanofibrous membrane via electrospinning for Cr(VI) ion removal from aqueous solution, *J. Environ. Manag.* 112 (2012) 10–16.
- [80] C.J. Li, Y.J. Li, J.N. Wang, J. Cheng, PA6@FexOy nanofibrous membrane preparation and its strong Cr(VI)-removal performance, *Chem. Eng. J.* 220 (2013) 294–301.
- [81] P. Kampalananwat and P. Supaphol, Preparation and Adsorption Behavior of Aminated Electrospun Polyacrylonitrile Nanofiber Mats for Heavy Metal Ion Removal, *ACS Appl. Mater. Interfaces* 2 (2010) 3619–3627.
- [82] A.A. Taha, J. Qiao, F. Li, B. Zhang, Preparation and application of amino functionalized mesoporous nanofiber membrane via electrospinning for adsorption of Cr³⁺ from aqueous solution, *J. Environ. Sci.* 24 (2012) 610–616.
- [83] M. Teng, H. Wang, F. Li, B. Zhang, Thioether-functionalized mesoporous fiber membranes: Sol-gel combined electrospun fabrication and their applications for Hg²⁺ removal, *J. Colloid Interface Sci.* 355 (2011) 23–28.
- [84] L. Zhang, J. Luo, T.J. Menkhaus, H. Varadaraju, Y. Sun, H. Fong, Antimicrobial nano-fibrous membranes developed from electrospun polyacrylonitrile nanofibers, *J. Membr. Sci.* 369 (2011) 499–505.
- [85] L. Camacho, L. Dumée, J. Zhang, J.-d. Li, M. Duke, J. Gomez, Advances in membrane distillation for water desalination and purification applications, *Water* 5 (2013) 94–196.
- [86] M. Khayet, T. Matsuura, Introduction to Membrane Distillation, in *Membrane Distillation*, Elsevier, Amsterdam, Chapter One, 1–16, 2011.
- [87] J.A. Prince, G. Singh, D. Rana, T. Matsuura, V. Anbharasi, T.S. Shanmugasundaram, Preparation and characterization of highly hydrophobic poly(vinylidene fluoride)—Clay nanocomposite nanofiber membranes (PVDF-clay NNMs) for desalination using direct contact membrane distillation, *J. Membr. Sci.* 397–398 (2012) 80–86.
- [88] J.A. Prince, D. Rana, G. Singh, T. Matsuura, T. Jun Kai, T.S. Shanmugasundaram, Effect of hydrophobic surface modifying macromolecules on differently produced PVDF membranes for direct contact membrane distillation, *Chem. Eng. J.* 242 (2014) 387–396.
- [89] J. Zhang, N. Dow, M. Duke, E. Ostarcevic, J.D. Li, S. Gray, Identification of material and physical features of membrane distillation membranes for high performance desalination, *J. Membr. Sci.* 349 (2010) 295–303.
- [90] C.Y. Feng, K.C. Khulbe, S. Tabe, Removal of volatile organic compound by membrane air stripping using electron-spun nanofiber membrane, *Desalination* 287 (2012) 98–102.
- [91] V. Thavasi, G. Singh, S. Ramakrishna, Electrospun nanofibers in energy and environmental applications, *Energy Environ. Sci.* 1 (2008) 205–221.
- [92] Y.C. Ahn, S.K. Park, G.T. Kim, Y.J. Hwang, C.G. Lee, H.S. Shin, J.K. Lee, Development of high efficiency nanofilters made of nanofibers, *Current App. Phys.* 6 (2006) 1030–1035.
- [93] A. Podgorski, A. Balazy, L. Gradon, Application of nanofibers to improve the filtration efficiency of the most penetrating aerosol particles in fibrous filters, *Chem. Eng. Sci.* 61 (2006) 6804–6815.
- [94] K. Kim, C. Lee, I. Kim, J. Kim, Performance modification of a melt-blown filter medium via an additional nano-web layer prepared by electrospinning, *Fibers Polym.* 10 (2009) 60–64.
- [95] N. Wang, X. Wang, B. Ding, J. Yu, G. Sun, Tunable fabrication of three-dimensional polyamide-66 nano-fiber/nets for high efficiency fine particulate filtration, *J. Mater. Chem.* 22 (2012) 1445–1452.